1-1-2014

Hierarchical porous Li 2 Mg(NH)2@C nanowires with long cycle life towards stable hydrogen storage

Guanglin Xia
University of Wollongong, gx168@uowmail.edu.au

Yingbin Tan
Fudan University

Dan Li
University of Wollongong, danli@uow.edu.au

Zaiping Guo
University of Wollongong, zguo@uow.edu.au

Hua-Kun Liu
University of Wollongong, hua@uow.edu.au

See next page for additional authors

Hierarchical porous Li 2 Mg(NH)2@C nanowires with long cycle life towards stable hydrogen storage

Abstract

The hierarchical porous $Li_2Mg(NH)_2$@C nanowires full of micropores, mesopores, and macropores are successfully fabricated via a single-nozzle electrospinning technique combined with *in-situ* reaction between the precursors, i.e., $MgCl_2$ and LiN_3, under physical restriction upon thermal annealing. The explosive decomposition of LiN_3 well dispersed in the electrospun nanowires during carbothermal treatment induces a highly porous structure, which provides a favourable way for H_2 delivering in and out of $Li_2Mg(NH)_2$ nanoparticles simultaneously realized by the space-confinement of the porous carbon coating. As a result, the thus-fabricated $Li_2Mg(NH)_2$@C nanowires present significantly enhanced thermodynamics and kinetics towards hydrogen storage performance, e.g., a complete cycle of H_2 uptake and release with a capacity close to the theoretical value at a temperature as low as 105°C. This is, to the best of our knowledge, the lowest cycling temperature reported to date. More interestingly, induced by the nanosize effects and space-confinement function of porous carbon coating, a excellently stable regeneration without apparent degradation after 20 de-/re-hydrogenation cycles at a temperature as low as 130°C was achieved for the as-prepared $Li_2Mg(NH)_2$@C nanowires.

Keywords

life, towards, stable, hydrogen, storage, porous, hierarchical, li, 2, mg, nh, c, nanowires, long, cycle

Disciplines

Engineering | Physical Sciences and Mathematics

Publication Details

Xia, G., Tan, Y., Li, D., Guo, Z., Liu, H., Liu, Z. & Yu, X. (2014). Hierarchical porous Li 2 Mg(NH)2@C nanowires with long cycle life towards stable hydrogen storage. Scientific Reports, 4 6599-1-6599-7. ACSMS

Authors

Guanglin Xia, Yingbin Tan, Dan Li, Zaiping Guo, Hua-Kun Liu, Zongwen Liu, and Xuebin Yu

SCIENTIFIC REPORTS

OPEN

CONFERENCE PROCEEDINGS

ACSMS2014

SUBJECT AREAS:
NANOWIRES
NANOPORES

Received
27 June 2014

Accepted
19 September 2014

Published
13 October 2014

Correspondence and requests for materials should be addressed to Z.G. (zguo@uow.edu.au) or X.Y. (yuxuebin@fudan.edu.cn)

Hierarchical Porous $Li_2Mg(NH)_2$@C Nanowires with Long Cycle Life Towards Stable Hydrogen Storage

Guanglin Xia[1,2], Yingbin Tan[2], Dan Li[1], Zaiping Guo[1], Huakun Liu[1], Zongwen Liu[3] & Xuebin Yu[2]

[1]Institute for Superconducting and Electronic Materials, University of Wollongong, Wollongong, Australia, [2]Department of Materials Science, Fudan University, Shanghai, China, [3]School of Chemical and Biomolecular Engineering, The University of Sydney, Sydney, Australia.

The hierarchical porous $Li_2Mg(NH)_2$@C nanowires full of micropores, mesopores, and macropores are successfully fabricated via a single-nozzle electrospinning technique combined with *in-situ* reaction between the precursors, i.e., $MgCl_2$ and LiN_3, under physical restriction upon thermal annealing. The explosive decomposition of LiN_3 well dispersed in the electrospun nanowires during carbothermal treatment induces a highly porous structure, which provides a favourable way for H_2 delivering in and out of $Li_2Mg(NH)_2$ nanoparticles simultaneously realized by the space-confinement of the porous carbon coating. As a result, the thus-fabricated $Li_2Mg(NH)_2$@C nanowires present significantly enhanced thermodynamics and kinetics towards hydrogen storage performance, e.g., a complete cycle of H_2 uptake and release with a capacity close to the theoretical value at a temperature as low as 105°C. This is, to the best of our knowledge, the lowest cycling temperature reported to date. More interestingly, induced by the nanosize effects and space-confinement function of porous carbon coating, a excellently stable regeneration without apparent degradation after 20 de-/re-hydrogenation cycles at a temperature as low as 130°C was achieved for the as-prepared $Li_2Mg(NH)_2$@C nanowires.

Solid-state hydrogen storage has been widely considered as the safest and most effective way to achieve the widespread use of H_2 as a prominent energy carrier in the future[1]. Despite decades of extensive efforts, it is still a big challenge to find a suitable H-rich material that features high safety, low cost, and fast kinetics for H_2 absorption and desorption under moderate conditions[2–4]. Metal-N-H systems have been extensively investigated as potential materials for solid-state hydrogen storage since the discovery of the hydrogen storage performance of the Li-N-H system, which was found to reversibly store 11.5 wt. % hydrogen[5,6]. Inspiringly, it was verified that partial substitution of Mg for Li in the Li-N-H composite to form the Li-Mg-N-H system could significantly decrease the desorption enthalpy change[7–9]. Among such composites, the $Mg(NH_2)_2$-2LiH system is one of the most promising hydrogen storage materials due to its favorable thermodynamics (39 kJ mol^{-1} H_2), which is lowered by 35% compared with the $LiNH_2$-LiH system, as well as its relatively high H_2 content and good reversibility[8–11]. According to the H_2 sorption process as described in Equation (1), 5.6 wt. % H_2 could be reversibly stored in this system at an operating temperature of 90°C under 1 bar of equilibrium hydrogen pressure, based on the thermodynamic calculation[12,13], which could satisfy the practical requirements of proton exchange membrane (PEM) fuel cells.

$$Li_2Mg(NH)_2 + 2H_2 \leftrightarrow Mg(NH_2)_2 + 2LiH \quad (1)$$

Nevertheless, due to both the sluggish interface reaction between $Mg(NH_2)_2$ and LiH in the preliminary step and the following mass transport across the thus-formed imide layer, which results in a rather high activation energy barrier (E_a: ~102–120 kJ mol^{-1}), a temperature higher than 200°C is required to achieve a reasonable H_2 sorption rate[13–15]. In addition, another big challenge for practical application of the Li-Mg-N-H system is the undesirable release of ammonia resulting from the insufficient reaction of $Mg(NH_2)_2$ with LiH, which not only significantly degrades the H_2 cycling capacity due to the loss of elemental N, but also would damage the active catalyst in the PEM fuel cells[16,17]. Previous experimental results have clearly established that, in terms of mitigating the above-mentioned problems, intimate contact between $Mg(NH_2)_2$ and LiH through the reduction of their

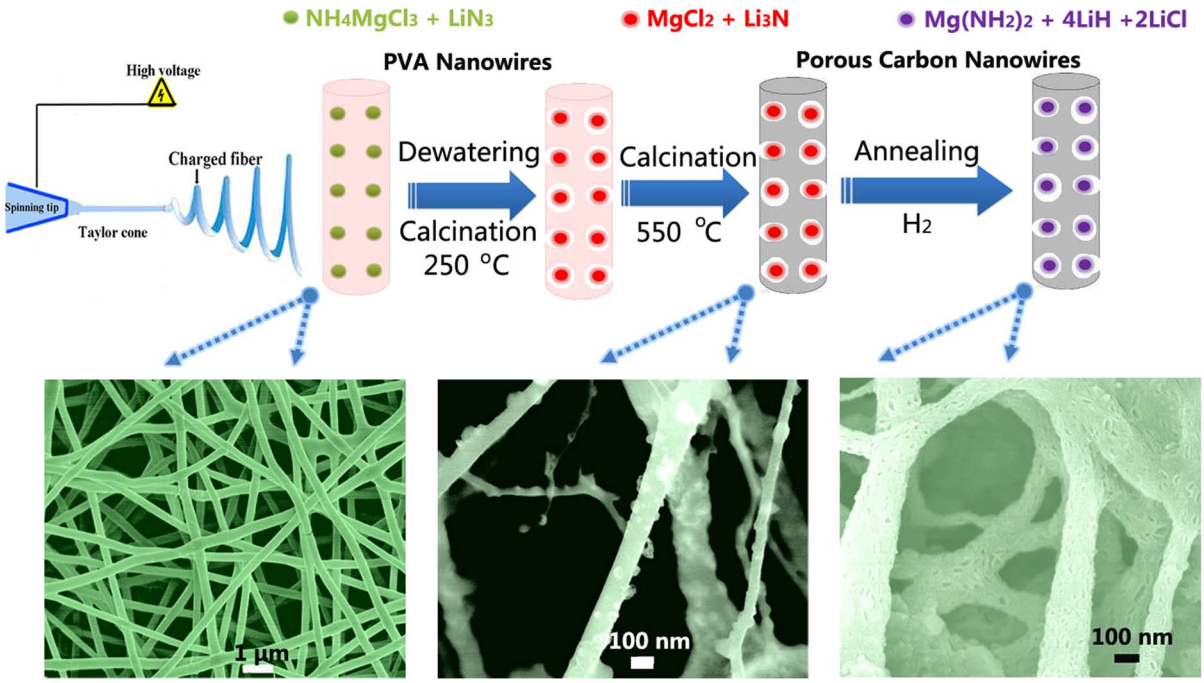

Figure 1 | **Schematic diagram of the in-situ technique to fabricate the carbon-coated Li-Mg-N-H NWs via electrospinning using a single-needle nozzle (top) and typical SEM images of the resulting products at different stages during preparation (bottom).**

particle sizes is an effective way of improving the hydrogen storage properties of the Li-Mg-N-H system[11,18]. It is well-known, however, that particles with small sizes are intrinsically unstable and prone to grow into larger crystallites[19]. Thus, during long-term cyclic heat treatment for H_2 release and uptake, phase separation and particle growth are inevitable, which would significantly degrade the sorption kinetics[19]. Therefore, an efficient host, which is both capable of uniformly confining the nanostructured morphology of the thus-synthesized complex hydrides during repeated heating and is chemically inert, is essential for preserving the nanosize effects on the active substrates inside.

To this end, nanoconfinement of complex hydrides in porous scaffolds, which can serve as containers, has emerged as an intriguing strategy to synthesize nanostructured materials and therefore improve their hydrogen storage properties[19–25]. The porous templates can effectively, on the one hand, facilitate the formation of nanoparticles and, on the other hand, maintain the shape and size of the active materials during cycles of hydrogen sorption[19]. In general, the preparation process involves melt infiltration or solution infiltration, which requires good wettability of the porous scaffolds by the precursors. Moreover, in order to achieve a relatively high loading level with good distribution, many repetitions of the infiltration steps and the following drying are required[26]. This makes the nanoconfinement time-consuming and tedious, while not allowing control over the homogeneous distribution of confined composites[26,27]. More importantly, the Li-Mg-N-H system is composed of multiphase components, and all of them have high chemical activity, low solubility, and/or high melting points, which therefore hinders the direct synthesis of a nanosized Li-Mg-N-H composite by the conventional nanoconfinement technique.

Herein, we report a novel *in-situ* reaction strategy based on an electrospinning technique, which is inexpensive, simple, and versatile, for the preparation of nanowoven materials, consisting of long entangled nanofibers of different materials, to fabricate nanowires (NWs) of Li-Mg-N-H composite uniformly coated with hierarchical porous carbon. As illustrated in Fig. 1, the overall synthetic procedure for the carbon-coated Li-Mg-N-H NWs originates from electrospinning coupled with the *in-situ* fabrication of the porous carbon coating and the consecutive transformation of the precursors to form the Li-Mg-N-H composite. Due to the special physicochemical properties of the components in the Li-Mg-N-H system, as mentioned above, our synthetic procedure is based on the *in-situ* reaction between $MgCl_2$ and LiN_3 as the electrospinning precursors. Upon heat treatment concurrent with carbonization to produce the uniform carbon coating, LiN_3 firstly decomposes into Li_3N with vigorous release of nitrogen, which then reacts with $MgCl_2$ to produce Mg_3N_2 via a metathesis reaction (2). With further increase of temperature, the interaction between the thus-formed Mg_3N_2 and the residual Li_3N results in the formation of disordered LiMgN-type structures (Fig. S1 and S2 in the Supporting Information)[28]. Afterwards, annealing under H_2 atmosphere induces the hydrogenation according to Equation (3)[29], which, as a result, forms the composite of $Mg(NH_2)_2$ and LiH, with LiCl as the by-product. The formation of $Mg(NH_2)_2$, LiH, and LiCl, as detected by X-ray diffraction of the bulk precursors after annealing (Fig. S1), could verify the feasibility of this procedure.

$$3MgCl_2 + 2Li_3N \rightarrow Mg_3N_2 + 6LiCl \quad (2)$$

$$Mg_3N_2 + 4Li_3N + 12H_2 \rightarrow 3Mg(NH_2)_2 + 12LiH \quad (3)$$

Results

Scanning electron microscope (SEM) images of the as-electrospun NWs are shown in Fig. 1. When a high voltage is applied between the outer metallic capillary, containing the mixed precursor solution of LiN_3, NH_4MgCl_3, and poly(vinyl alcohol) (PVA), and the collector, the liquid jets are stretched by electrostatic forces to generate textile NWs with a uniform coating of PVA. From the SEM images, the formation of a highly interconnected network of the as-electrospun NWs with a diameter of ~250 nm is clearly observed. Subsequently, the as-collected NWs were dewatered at ~85°C, and the temperature was then programmed to rise to 250°C under dynamic vacuum, meanwhile realizing the transformation of NH_4MgCl_3 into $MgCl_2$,

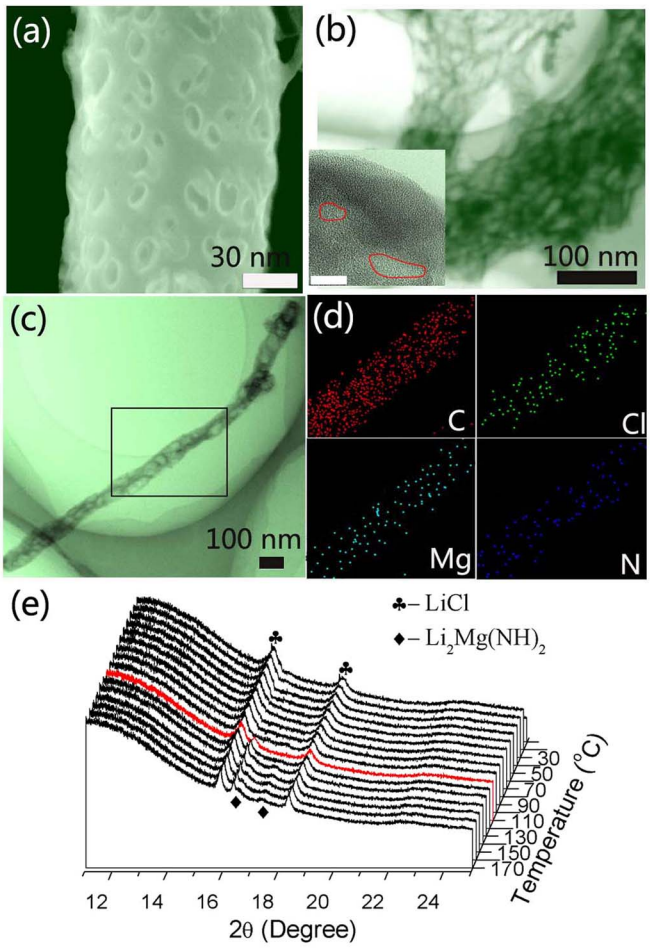

Figure 2 | (a) High-magnification SEM image of a single Li-Mg-N-H NW; (b) TEM image of Li-Mg-N-H NWs (inset: high-magnification TEM image (scale bar 5 nm), in which the marked area clearly shows the small and large mesopores coated with carbon). TEM image (c) and the corresponding elemental mapping (d) of the as-prepared Li-Mg-N-H NWs with nanoconfinement of the precursors. (e) High-resolution XRD spectra of the Li-Mg-N-H NWs upon heating to various temperatures.

accompanied by the release of the thus-formed ammonia and hydrogen chloride. Simultaneously, the formation of Li_3N due to the decomposition of LiN_3 was verified by the color change (Fig. S3) to the characteristic color of Li_3N, *i.e.*, ruby red from white, across this heating step. On elevating the calcination temperature to 550°C under N_2 atmosphere, the PVA substrates were then transformed into pyrolysis carbon upon thermal decomposition, which homogeneously puts "carbonaceous clothes" on the active composite inside, accompanied by the metathesis reaction between $MgCl_2$ and Li_3N. As shown in Fig. 1, the carbonized NWs perfectly maintain the structural integrity of the as-electrospun polymers and, compared to polymeric NWs with smooth surfaces, exhibit rough surfaces with small relics and mesoporous structure on the outside wall. This is supposed to stem from the explosive release of N_2 during the decomposition of LiN_3, which could push away the surrounding PVA substrate from the point where LiN_3 exists, leading to the formation of numerous pores after the carbonization of relatively flexible polymers into relatively stiff carbon sheets at high temperature[27]. Magnified images of Li-Mg-N-H NWs (Fig. 2a) can further demonstrate the presence of open pores on the external surface, with pore diameters in the range of 2–40 nm. It also was found that the diameter of the as-electrospun PVA NWs was significantly decreased after carbonization, due to the decomposition of the polymer during calcination[30]. In the high-resolution transmission electron microscope (HRTEM) image (Fig. 2b), not only the wirelike nanostructure, but also the porous interior with mesopores and macropores can be clearly observed. This verifies the homogenous distribution of pores, which can effectively facilitate the H_2 transportation across the carbon matrix, owing to the explosive decomposition of LiN_3 inside the carbonized wires, indirectly confirming the uniform dispersion of Li-Mg-N-H composite. The HRTEM image (inset of Fig. 2b) also reveals the presence of small mesopores (~2.5 nm) inside the disordered carbon sheets. The N_2 adsorption-desorption isotherms of the as-prepared NWs exhibit typical type-IV hysteresis, with an obvious increase at a high relative pressure (P/P_o = 0.80–0.99), indicative of the presence of both macropores and mesopores, due to the compression of PVA by the strong power of the N_2 stream and the subsequent solidification from carbonization, which agrees well with the TEM results. In addition, the isotherms show increases in adsorption at a low relative pressure, suggesting the presence of a large number of micropores in the NWs after calcination. These pores may be derived from the free volume and microporosity in the carbon NWs that is attributed to the disordered packing of the turbostratic carbon sheets and clusters as a result of the carbonization process of the nanostructured polymers[31–33]. Taking advantage of the one-dimensional (1D) and hierarchical porous architecture, the $Li_2Mg(NH)_2$@C possesses a relatively large Brunauer-Emmett-Teller (BET) surface area of around 438 $m^2\ g^{-1}$ and pore volume of 0.86 $cm^3\ g^{-1}$ according to the N_2 sorption isotherms (Fig. S4). Moreover, the pore size distribution further demonstrates the formation of mesopores in the as-prepared NWs. Accordingly, on account of the special physico-chemical properties of every individual component in the as-electrospun matrices, the hierarchical porous carbon NWs can be obtained via a simple single-nozzle electrospinning. It is worth noting that the energy dispersive spectroscopy (EDS) elemental map (Fig. 2d) of C coincides well with the structure of the NWs, while the maps of Cl, Mg, and N agree well with the C map, which directly demonstrates the homogeneous dispersion of the precursors inside the carbon NWs.

After the carbothermal treatment and annealing in the H_2 atmosphere, high-resolution X-ray diffraction (HRXRD) verified the formation of LiCl, as shown in Fig. 2e, while other products are undiscernible due to a lack of long-range order. The characteristic peaks assigned to the N-H bonds of $Mg(NH_2)_2$ can be clearly detected, however, from the Fourier transform infrared (FTIR) spectra (Fig. S5), indicating the presence of $Mg(NH_2)_2$ embedded in the porous NWs. Moreover, the *in-situ* HRXRD confirms the generation of $Li_2Mg(NH)_2$ with increasing temperature, providing direct evidence of the successful synthesis of the porous carbon-coated $Li_2Mg(NH)_2$ NWs. In addition, the surrounding carbon matrix appears to have an amorphous structure, acting as a strong buffer to accommodate the sintering of nanostructured $Li_2Mg(NH)_2$ during the cycles of H_2 sorption. As deduced from the Debye-Scherrer equation, the average crystallite size of the carbon-coated $Li_2Mg(NH)_2$ is only ~4 nm. Clearly, the electrospinning will, on the one hand, eliminate the tedious process of infiltration and drying and, at the same time, is suitable for good encapsulation and distribution of the precursors inside the as-electrospun NWs[34], while the blocking of pores and/or agglomeration of active composite on the outside surface of the templates is usually observed during nanoconfinement, which significantly limits complete pore filling and good dispersion of complex hydrides inside the scaffolds[26]. Finally, the *in-situ* metathesis reaction between $MgCl_2$ and Li_3N stemming from the well-dispersed precursors inside the thus-formed carbon NWs, followed by the hydrogenation process, leads to the formation of the nanosized Li-Mg-N-H composite with homogeneous distribution. Therefore, as a result of the explosive release of N_2 from the as-electrospun wires upon carbothermal treatment, the obtained car-

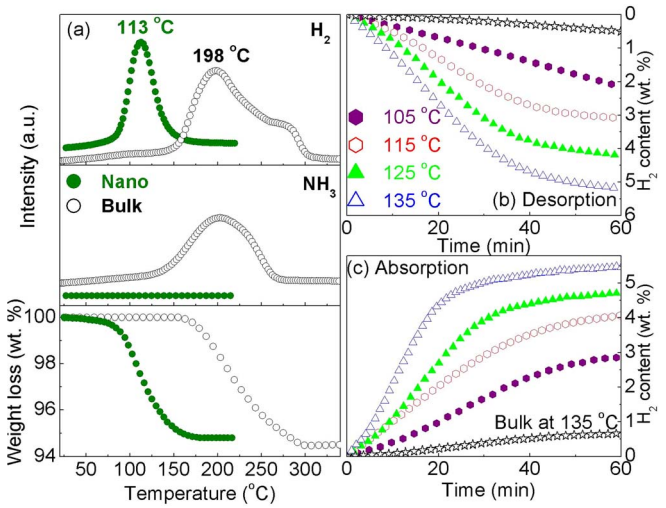

Figure 3 | (a) Mass spectra (top) and thermogravimetry curves (bottom) of the carbon-coated Li-Mg-N-H NWs and bulk $Mg(NH_2)_2$/2LiH composite after complete hydrogenation. Hydrogen desorption (b) and absorption (c) curves of the carbon-coated Li-Mg-N-H NWs at different temperatures, with the ball-milled $Mg(NH_2)_2$/2LiH composite at 135°C included for comparison. Carbon was not considered as an active component for the hydrogen storage measurements.

bon-coated Li-Mg-N-H-based NWs possess a well-designed 1D nanostructure and a three-dimensional (3D) interconnected texture full of micropores, mesopores, and macropores, which can effectively hinder the growth and agglomeration of the confined nanoparticles during heat treatment and promote H_2 access through the porous carbonaceous framework to interact with the active substrates. This is the first report, to the best of our knowledge, on the *in-situ* synthesis of a carbon-coated Li-Mg-N-H-based system with 3D porous nanostructures.

To compare the dehydrogenation behavior of the Li-Mg-N-H-based NWs with that of a ball-milled composite of $Mg(NH_2)$/2LiH, mass spectrometry (MS), thermogravimetry (TG), and volumetric temperature-programmed desorption (TPD) characterizations were conducted, as shown in Fig. 3. The bulk Li-Mg-N-H system after ball milling starts to dehydrogenate above 140°C, with dehydrogenation peaking at ~199°C, along with the simultaneous emission of ammonia, which is generally consistent with reports in the literature[35–41]. In comparison, the carbon-coated Li-Mg-N-H NWs exhibited onset and peak temperatures of H_2 desorption that were downshifted to ~78°C and 113°C, respectively, which are 62°C and 86°C lower, respectively, than for their ball-milled counterpart. It is also noteworthy that the generation of the toxic by-product, *i.e.*, NH_3, was significantly depressed in the thermal dehydrogenation of the Li-Mg-N-H NWs, which is favorable for both reversibility and onboard practical applications as a hydrogen-storage medium. The quantitative H_2 desorption measurement by the TG method confirmed the dramatically reduced operating temperature of the carbon-coated Li-Mg-N-H NWs, which corresponds well with the MS spectra. A weight loss of 5.5 wt. % H_2 could be achieved in the temperature range between 78°C and 155°C. From the *in-situ* HRXRD results (Fig. 2e), the formation of $Li_2Mg(NH)_2$ upon dehydrogenation is confirmed to start at a temperature of ~110°C, which is consistent with the TG-MS results.

The isothermal H_2 desorption and absorption properties (Fig. 3b, c) were further characterized by volumetric measurements to clarify the effects of both the reduction in the particle size and the carbonaceous coating with highly porous nanostructure on the modification of the Li-Mg-N-H system. The ball-milled composite shows a H_2 capacity of approximately 0.5 wt. % and 0.65 wt. % for desorption and absorption, respectively, within 60 min, even at the high temperature of 135°C. On the contrary, the carbon-coated Li-Mg-N-H NWs display a fast hydrogenation at 135°C, with a capacity reaching up to 5.5 wt. %, and a subsequent hydrogen release as high as ~5.2 wt. % can be implemented over the period of 60 min. In particular, upon decreasing the operating temperature to 105°C, the H_2 sorption from the Li-Mg-N-H NWs can still proceed, and a complete cycle of H_2 uptake and release (~5.5 wt. %) can be achieved with an extended holding time (Fig. S6). In order to quantitatively estimate the enormously enhanced hydriding/dehydriding kinetics for the as-prepared carbon-coated Li-Mg-N-H NWs, the apparent activation energies (E_a) during the H_2 absorption/desorption were determined by combining the Johnson-Mehl-Avrami equation with the Arrhenius equation after fitting the experimental results at various temperatures. Based on the slope of the linear plots of ln (k) (k, rate constant) versus $1/T$ (T, absolute temperature), the activation energy for hydrogenation and dehydrogenation of the porous carbon-coated Li-Mg-N-H NWs was verified to be around 23.9 and 24.5 kJ mol^{-1} H_2, respectively, very much lower than for the bulk counterpart (Fig. S7). This directly confirms the significant enhancement of kinetics for the carbon-coated Li-Mg-N-H NWs, due to the reduction of particle size and therefore diffusion distances.

Another important issue with Li-Mg-N-H composite for hydrogen storage application is the significant degradation of H_2 capacity upon cycling, owing to the release of ammonia, and the particle growth and phase separation during thermal treatment. The cycling behaviour of the carbon-coated Li-Mg-N-H NWs, in comparison with their bulk counterpart, is shown in Fig. 4 and Fig. S8, using isothermal dehydrogenation and hydrogenation. The H_2 capacity, as cycling of the bulk Li-Mg-N-H composite proceeds, is severely degraded from 0.7 wt. % to 0.35 wt. % after only 5 cycles of sorption, which is equal to a capacity retention lower than 50%, even with a dwell time of 400 min for one cycle at 130°C. In contrast, in the case of the carbon-coated Li-Mg-N-H NWs cycled under the same conditions, but over a significantly shorter time, the H_2 capacity still reaches 5.3 wt. % and the capacity retention is up to 94.6% after 20 consecutive cycles of hydrogenation and dehydrogenation. The characteristic peaks of $Mg(NH_2)_2$ and $Li_2Mg(NH)_2$ can be clearly observed, even through 20 cycles of sorption (Fig. S9), and the porous structure of the $Li_2Mg(NH)_2$@C NWs is well maintained after cyclic heat treatment (Fig. S10). Furthermore, the curves of absorption and desorption during the cyclic H_2 sorption are almost identical to each other (Fig. S11), indicating the greatly enhanced hydrogen storage performance, *i.e.*, capacity and kinetics were well-preserved, which is attributed to a strong tolerance of the porous carbonaceous coating towards particle growth and sintering.

Discussion

It is well known that the high activation energy barriers for both the hydrogenation and the dehydrogenation of the Li-Mg-N-H composite results from the sluggish interface reaction due to the slow diffusion of atoms (e.g., Li^+, Mg^{2+}, and H^+ ions) across amide-imide and imide-hydride phase boundaries and the mass transport along the as-formed layer of imides[18,42]. The reduction of particle size into nanometer range can significantly decrease the diffusion pathways across amides/imides and hydrides, increase their surface area and develop closer proximity between $Mg(NH_2)_2$ and LiH, which would lead to the significantly improved kinetics and thermodynamics towards superior hydrogen storage performance. In the case of the ball-milled Li-Mg-N-H composite, the sizes of most of the particles are larger than 1 μm (Fig. S12), and therefore, the surface-to-volume ratio is small, which endows it with high activation energy. By contrast, it is notable that the *in-situ* fabrication of the carbon-coated $Li_2Mg(NH)_2$ via electrospinning followed by calcination and annealing can, on the one hand, realize the direct synthesis of nanosized $Li_2Mg(NH)_2$ (~4 nm), significantly improving its hydrogen storage

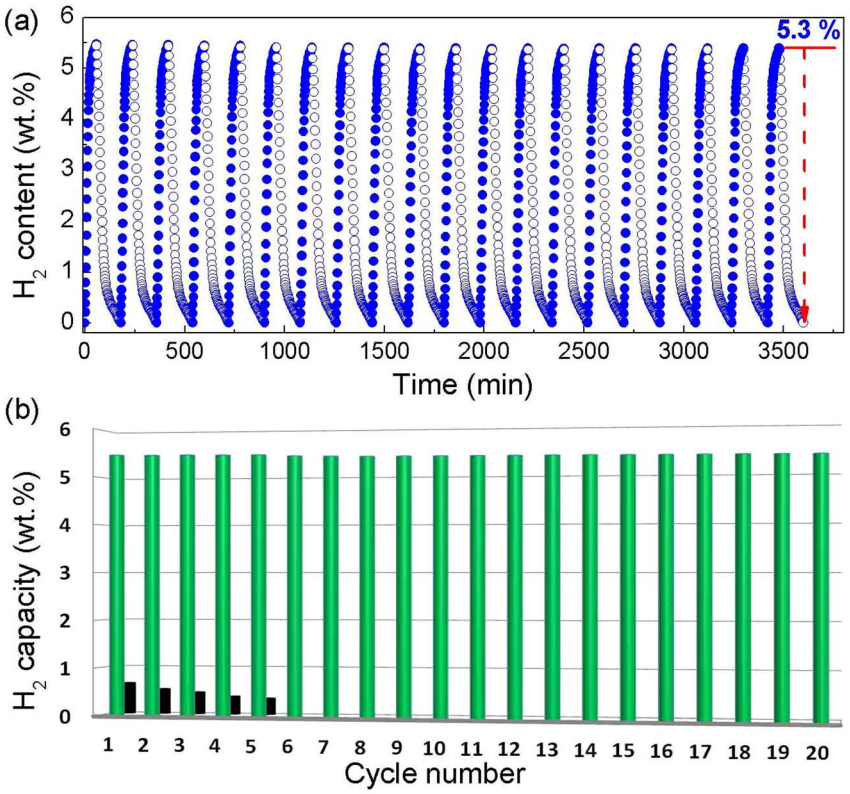

Figure 4 | (a) Reversible H_2 sorption performance of the carbon-coated Li-Mg-N-H NWs at 130°C, and (b) H_2 capacity dependence of the carbon-coated Li-Mg-N-H NWs (green) and their ball-milled counterpart (black) on cycle number.

performance (Fig. 3), while, on the other hand, the space-confinement function of the porous carbon coating can well preserve the nanostructural features down to the nanometer scale during consecutive cycles of heating, which therefore gives the $Li_2Mg(NH)_2$ stable reversibility without apparent degradation, even up to 20 cycles of de-/re-hydrogenation (Fig. 4).

In summary, we have successfully prepared hierarchically porous $Li_2Mg(NH)_2$@C NWs *via* a simple and scalable single-nozzle electrospinning technique with a subsequent carbothermal reaction, which realizes the *in-situ* formation of a porous carbon coating serving as template, with the Li-Mg-N-H composite produced via the subsequent reaction under physical restriction. Our results obviously verified the significantly improved hydrogen storage performance, including complete reversibility at a temperature as low as 105°C and tremendous reduction of the hydriding/dehydriding temperature of the $Li_2Mg(NH)_2$, with the reduction of particle size down to the nanometer scale. Induced by the space-confinement of the porous carbon coating, the $Li_2Mg(NH)_2$@C NWs present very good cycling stability, close to the theoretical value over 20 cycles of de-/re-hydrogenation at 130°C. To the best of our knowledge, no such highly stable cycling at relatively low temperature has been reported for Li-Mg-N-H based materials. However, it should be noted that, due to the extra weight of the porous carbon NWs and the by-product of LiCl , the actual reversible H_2 capacity in the whole system is limited. Therefore, further works in the search of an effective solvent to remove the inactive LiCl and/or a new synthetic strategy to achieve a high loading percent of precursors are still required to achieve a high hydrogen storage capacity in the whole system. Nonetheless, these results demonstrate the potential of this strategy in further improving the hydrogen storage performance of complex hydrides and designing the nanowire-like structure with a wide range of materials for developing high-performance energy storage applications.

Methods

Synthesis of hierarchical porous $Li_2Mg(NH)_2$@C nanowires. Poly(vinyl alcohol) (PVA, 0.5 g, Alfa Aesar, M_v = 88000, CAS: 9002-89-5) was mixed with deionized water (5 mL) and stirred in a water bath at 90°C for 8 h to make the PVA solution. After cooling down to room temperature, LiN_3 solution (0.5 mL, 20 wt. %) and NH_4MgCl_3 (0.05 g) in water were then added and vigorously stirred for 6 h to make a homogeneous spinning dope. The resultant precursor solution was poured into a syringe with a 18-gauge blunt tip needle. The flow rate of the solution was approximately 500 μL h^{-1} and was controlled by a syringe pump (Longer, TJP-3A, China). A grounded stainless steel plate was horizontally placed 10 cm from the needle to collect the as-electrospun NWs. A high voltage of 15 kV was applied by a high-voltage power supply. The as-collected electrospun nanowires were firstly dewatered at a temperature of 85°C under dynamic vacuum for 15 h and then calcined at 550°C for 3 h under dynamic N_2 atmosphere to obtain the porous carbon NWs containing the precursors (heating rate 1°C min^{-1}). Finally, the thus-formed carbon NWs were annealed under 150 bar H_2 at 300°C for 12 h for a complete hydrogenation, as schematically illustrated in Fig. 1, and then further annealed under vacuum for dehydrogenation at 150°C, which leads to the formation of the hierarchically porous $Li_2Mg(NH)_2$@C NWs. According to elemental analysis, the resulting nanowires contained 9.86 mass% Li, 5.7 mass% Mg, 6.23 mass% N, 2.8 mass% O, 16.7 mass% Cl, and 58.5 mass% C, which gives the mass concentration of $Li_2Mg(NH)_2$ of ~15.2 mass% in the as-prepared carbon NWs.

Preparation of the ball-milled composite. The ball-milling of $Mg(NH_2)_2$ and LiH with a molar ratio of 1 : 2 was conducted via a planetary QM-1SP2 for 10 h. The ball-to-powder ratio was 30 : 1, with a milling speed of 500 rpm. The milling procedure was carried out by alternating between 30 min of milling and 6 min of rest. In order to prevent contamination by air, all handling and manipulation of the materials were performed in an argon-filled glove box with a recirculation system to keep H_2O and O_2 levels below 1 ppm.

Materials characterization. Mass spectrometry (MS; Hidden HPR 20) was conducted from room temperature, using a heating rate of 2°C min^{-1} under dynamic nitrogen with a purge rate of 80 ml min^{-1}. Differential scanning calorimetry (DSC) measurements were performed with a TAQ 2000 DSC under N_2 with a gas flow of 40 mL min^{-1} at a heating rate of 2°C min^{-1}. Nitrogen absorption/desorption isotherms (Brunauer-Emmett-Teller (BET) technique) at the temperature of liquid nitrogen via a Quantachrome NOVA 4200e instrument were collected to characterize the pore structure of the samples. The pore volumes and pore size distributions were obtained by using the Barrett-Joyner-Halenda (BJH) model from the adsorption branches of isotherms. The phase composition of the powders was analyzed by X-ray

diffraction (XRD, D8 Advance, Bruker AXS) with Cu Kα radiation. Amorphous tape was used to prevent any possible reactions between the sample and air during the XRD measurement. High-resolution X-ray diffraction data were collected by a Mythen-II detector at the Powder Diffraction Beamline, Australian Synchrotron. The sample was loaded into a pre-dried 0.7 mm boron-silica glass capillary tube, and the capillary tube was then sealed with vacuum grease in a glove box filled with argon. In order to identify the phase transformations during dehydrogenation, time-resolved *in-situ* measurements were conducted using a Cyberstar hot-air blower to heat the capillary from room temperature to the desired temperature, at a constant heating rate of 2°C min^{-1}. Fourier transform infrared (FTIR, Magna-IR 550 II, Nicolet) analysis was conducted to determine the chemical bonding. During the FTIR measurements (KBr pellets), samples were loaded into a closed tube with KBr for measurement in an argon-filled glove box. The morphology of the samples was evaluated using a field emission scanning electron microscope (FE-SEM, JEOL 7500FA, Tokyo, Japan) and a transmission electron microscope (TEM, JEOL 2011 F, Tokyo, Japan). Elemental analysis was performed with an Elemen Tar Vario EL3 Elemental Analyser.

The hydrogen storage properties of the thus-synthesized $Li_2Mg(NH)_2$@C NWs were investigated on a Sievert's apparatus, denoted as a gas reaction controller (GRC, Advanced Materials Corp., USA). The apparatus was carefully calibrated from the H_2 sorption of a $LaNi_5$ reference sample with an accuracy of ±1%, and, typically, a ~800 mg sample was loaded into a stainless-steel autoclave for hydrogenation and dehydrogenation measurements. The H_2 absorption kinetics measurements were performed at various temperatures with an initial pressure of 35 atm, and the desorption properties were detected at various temperatures under a hydrogen pressure below 0.02 atm. The pressure-concentration isotherm (PCI) measurements were performed at the desired temperatures, and the equilibrium time for each point was 600 s. For comparison purposes, the carbon scaffold masses were excluded when determining the amount of hydrogen released from the relevant composites containing carbon scaffolds.

1. Schlapbach, L. & Zuttel, A. Hydrogen-storage materials for mobile applications. *Nature* **414**, 353–358 (2001).
2. Orimo, S.-i., Nakamori, Y., Eliseo, J. R., Züttel, A. & Jensen, C. M. Complex hydrides for hydrogen storage. *Chem. Rev.* **107**, 4111–4132 (2007).
3. Grochala, W. & Edwards, P. P. Thermal decomposition of the non-interstitial hydrides for the storage and production of hydrogen. *Chem. Rev.* **104**, 1283–1315 (2004).
4. Klerke, A., Christensen, C. H., Norskov, J. K. & Vegge T. Ammonia for hydrogen storage: challenges and opportunities. *J. Mater. Chem.* **18**, 2304–2310 (2008).
5. Chen, P., Xiong, Z. T., Luo, J. Z., Lin, J. Y. & Tan, K. L. Interaction of hydrogen with metal nitrides and imides. *Nature* **420**, 302–304 (2002).
6. Xie, L., Zheng, J., Liu, Y., Li, Y. & Li, X. G. Synthesis of Li_2NH hollow nanospheres with superior hydrogen storage kinetics by plasma metal reaction. *Chem. Mater.* **20**, 282–286 (2007).
7. Leng, H. Y., Ichikawa, T., Hino, S., Nakagawa, T. & Fujii, H. Mechanism for hydrogenation reaction in the Li-Mg-N-H system. *J. Phys. Chem. B* **109**, 10744–10748 (2005).
8. Xiong, Z. T., Wu, G. T., Hu, H. J. & Chen, P. Ternary imides for hydrogen storage. *Adv. Mater.* **16**, 1522–1525 (2004).
9. Leng, H., Ichikawa, T. & Fujii, H. Hydrogen storage properties of Li-Mg-N-H systems with different ratios of $LiH/Mg(NH_2)_2$. *J. Phys. Chem. B* **110**, 12964–12968 (2006).
10. Liu, Y. F., Hu, J., Wu, G., Xiong, Z. & Chen, P. Formation and equilibrium of ammonia in the $Mg(NH_2)_2$-2LiH hydrogen storage system. *J. Phys. Chem. C* **112**, 1293–1298 (2008).
11. Liu, Y. F. *et al.* Size-dependent kinetic enhancement in hydrogen absorption and desorption of the Li-Mg-N-H system. *J. Am. Chem. Soc.* **131**, 1862–1870 (2009).
12. Luo, W. ($LiNH_2$-MgH_2): a viable hydrogen storage system. *J. Alloys Compd.* **381**, 284–287 (2004).
13. Xiong, Z. T. *et al.* Thermodynamic and kinetic investigations of the hydrogen storage in the Li-Mg-N-H system. *J. Alloys Compd.* **398**, 235–239 (2005).
14. Chen, P., Xiong, Z. T., Yang, L. F., Wu, G. T. & Luo, W. F. Mechnistic investigations on the heterogeneous solid-state reaction of magnesium amides and lithium hydrides. *J. Phys. Chem. B* **110**, 14221–14225 (2006).
15. Sudik, A., Yang, J., Halliday, D. & Wolverton, C. Kinetic improvement in the $Mg(NH_2)_2$-LiH storage system by product seeding. *J. Phys. Chem. C* **111**, 6568–6573 (2007).
16. Liang, C. *et al.* Li-Mg-N-H-based combination systems for hydrogen storage. *J. Alloys Compd.* **509**, 7844–7853 (2011).
17. Ikeda, S., Tokoyoda, K., Kiyobayashi, T. & Kuriyama, N. Cyclic properties and ammonia by-product emission of Li/Mg-N-H hydrogen storage materials. *Int. J. Hydrogen Energy* **36**, 8373–8380 (2011).
18. Xie, L., Liu, Y., Li, G. & Li, X. G. Improving hydrogen sorption kinetics of the $Mg(NH_2)_2$-LiH system by the tuning particle size of the amide. *J. Phys. Chem. C* **113**, 14523–14527 (2009).
19. de Jongh, P. E., Allendorf, M., Vajo, J. J. & Zlotea, C. Nanoconfined light metal hydrides for reversible hydrogen storage. *MRS Bull.* **38**, 488–494 (2013).
20. Reardon, H. *et al.* Emerging concepts in solid-state hydrogen storage: the role of nanomaterials design. *Energy Environ. Sci.* **5**, 5951–5979 (2012).
21. Nielsen, T. K., Besenbacher, F. & Jensen, T. R. Nanoconfined hydrides for energy storage. *Nanoscale*, **3**, 2086–2098 (2011).
22. Nielsen, T. K. *et al.* A reversible nanoconfined chemical reaction. *ACS Nano* **4**, 3903–3908 (2010).
23. Adelhelm, P. & de Jongh, P. E. The impact of carbon materials on the hydrogen storage properties of ligh metal hydrides. *J. Mater. Chem.* **21**, 2417–2427 (2011).
24. Xia, G. L. *et al.* Nanoconfinement significantly improves the thermodynamics and kinetics of co-infiltrated $2LiBH_4$-$LiAlH_4$ composites: stable reversibility of hydrogen absorption/resorption. *Acta Mater.* **61**, 6882–6893 (2013).
25. Xia, G. L. *et al.* Stabilization of $NaZn(BH_4)_3$ via nanoconfinement in SBA-15 towards enhanced hydrogen release. *J. Mater. Chem. A* **1**, 250–257 (2013).
26. Christian, M. L. & Aguey-Zinsou, K.-F. Core-shell strategy leading to high reversible hydrogen storage capacity for $NaBH_4$. *ACS Nano* **6**, 7739–7751 (2012).
27. Xia, G. L. *et al.* Carbon-coated Li_3N nanofibers for advanced hydrogen storage. *Adv. Mater.* **25**, 6238–6244 (2013).
28. Yamane, H., Okabe, T. H., Ishiyama, O., Waseda, Y. & Shimada, M. Ternary nitrides prepared in the Li_3N-Mg_3N_2 system at 900-1000 K. *J. Alloys Compd.* **319**, 124–130 (2001).
29. Nakamori, Y., Kitahara, G., Miwa, K., Towata, S. & Orimo, S. Reverisble hydrogen-storage functions for mixtures of Li_3N and Mg_3N_2. *Appl. Phys. A* **80**, 1–3 (2005).
30. Zhang, F. *et al.* Flexible films derived from electrospun carbon nanofibers incorporated with Co_3O_4 hollow nanoparticles as self-surpported elctrodes for electrochemical capacitors. *Adv. Funct. Mater.* **23**, 3909–3915 (2013).
31. Ouyang, Y., Shi, H., Fu, R. & Wu, D. Highly monodisperse microporous polymeric and carbonaceous nanospheres with multifunctional properties. *Sci. Rep.* **3**, 1430; doi:10.1038/srep1430 (2013).
32. Liang, Y., Wu, D. & Fu, R. Carbon microfibers with hierarchical porous structure from electrospun fiber-like natural biopolymer. *Sci. Rep.* **3**, 1119; doi:10.1038/srep01119 (2013).
33. Wu, D. *et al.* Design and preparation of porous polymers. *Chem. Rev.* **112**, 3959–4015 (2012).
34. Wu, J., Wang, N., Zhao, Y. & Jiang, L. Electrospinning of multilevel structured functional micro-/nanofiberes and their applications. *J. Mater. Chem. A* **1**, 7290–7305 (2013).
35. Pan, H. *et al.* Improved hydrogen storage kinetics of the Li-Mg-N-H system by addition of $Mg(BH_4)_2$. *Dalton Trans.* **42**, 3802–3811 (2013).
36. Liu, Y., Li, C., Li, B., Gao, M. & Pan, H. Metathesis reaction-induced significant improvement in hydrogen storage properties of the KF-added $Mg(NH_2)_2$-2LiH system. *J. Phys. Chem. C* **117**, 866–875 (2013).
37. Liang, C., Liu, Y., Gao, M. & Pan, H. Understanding the role of K in the significantly improved hydrogen storage properties of a KOH-doped Li-Mg-N-H system. *J. Mater. Chem. A* **1**, 5031–5036 (2013).
38. Li, B., Liu, Y., Gu, J., Gao, M. & Pan, H. Synergetic effects of in situ formed CaH_2 and $LiBH_4$ on hydrogen strorage properties of the Li-Mg-N-H system. *Chem. Asian J.* **8**, 374–384 (2013).
39. Li, B., Liu, Y., Zhang, Y., Gao, M. & Pan, H. Reaction pathways for hydrogen uptake of the Li-Mg-N-based hydrogen storage system. *J. Phys. Chem. C* **116**, 13551–13558 (2012).
40. Liu, Y. *et al.* Correlation between composition and hydrogen storage behaviors of the Li_2NH-MgNH combination system. *Dalton Trans.* **40**, 8179–8186 (2011).
41. Wang, J. *et al.* Potassium-modified $Mg(NH_2)_2$/2LiH system for hydrogen storage. *Angew. Chem. Int. Ed.* **48**, 5828–5832 (2009).
42. Akbarzadeh, A. R., Ozolins, V. & Wolverton, C. First-principles determination of multicomponent hydride phase diagrams: application to the Li-Mg-N-H system. *Adv. Mater.* **19**, 3233–3239 (2007).

Acknowledgments

This work was partially supported by the Ministry of Science and Technology of China (2010CB631302), the National Natural Science Foundation of China (21271046), the PhD Programs Foundation of the Ministry of Education of China (20110071110009), and the Science and Technology Commission of Shanghai Municipality (11JC1400700). Z. Guo acknowledges a University Research Committee (URC) grant from the University of Wollongong financial support provided by the Australian Research Council (ARC) through an ARC Discovery Project (DP140102858). Part of this research was undertaken on the Powder Diffraction Beamline at the Australian Synchrotron, Victoria, Australia. The authors also would like to thank Dr. Tania Silver for critical reading of the manuscript.

Author contribution

G.L.X., Z.P.G., H.K.L. and X.B.Y. proposed, planned, and designed the project. G.L.X., Y.B.T., D.L. and Z.W.L. performed the material preparation, characterizations, and hydrogen storage tests. All authors contributed to writing the manuscript.

Additional information

Supplementary information accompanies this paper at http://www.nature.com/scientificreports

Competing financial interests: The authors declare no competing financial interests.

How to cite this article: Xia, G.L. *et al*. Hierarchical Porous $Li_2Mg(NH)_2$@C Nanowires with Long Cycle Life Towards Stable Hydrogen Storage. *Sci. Rep.* **4**, 6599; DOI:10.1038/srep06599 (2014).